ETS1 transcriptional activity is increased in advanced prostate cancer and promotes the castrate-resistant phenotype

A.M.Smith, V.J.Findlay, S.G.Bandurraga,
E.Kistner-Griffin[1], L.S.Spruill, A.Liu[2], A.R.Golshayan[3]
and D.P.Turner[*]

Department of Pathology and Laboratory Medicine, [1]Department of
Medicine, [2]Hollings Cancer Center and [3]Division of Hematology and
Oncology, Medical University of South Carolina, Charleston, SC 29425, USA

[*]To whom correspondence should be addressed. Walton Research Building,
Room RS308, Medical University of South Carolina, 39 Sabin Street,
Charleston, SC 29425, USA. Tel: +1 843 792 8011; Fax: +1 843 792 2666;
Email: turnerda@musc.edu

Advanced disease accounts for the majority of prostate cancer-related deaths and androgen deprivation therapy (ADT) is the standard of care for these patients. Many patients undergoing ADT become resistant to its effects and progress to castrate-resistant prostate cancer (CRPC). Current therapies for CRPC patients are inadequate, with progression-free survival rates as low as 2 months. The molecular events that promote CRPC are poorly understood. ETS (v-ets erythroblastosis virus E26 oncogene) transcription factors are regulators of carcinogenesis. Protein levels of the archetypical ETS factor, ETS1, are increased in clinical and latent prostate cancer relative to benign prostatic hyperplasia and normal prostate to promote multiple cancer-associated processes, such as energy metabolism, matrix degradation, survival, angiogenesis, migration and invasion. Our studies have found that ETS1 expression is highest in high-grade prostate cancer (Gleason 7 and above). Increased ETS1 expression and transcriptional activity promotes an aggressive and castrate-resistant phenotype in immortalized prostate cancer cells. Elevated AKT (v-akt murine thymoma viral oncogene homolog) activity was demonstrated to increase ETS1 protein levels specifically in castrate-resistant cells and exogenous ETS1 expression was sufficient to rescue invasive potential decreased by inhibition of AKT activity. Significantly, targeted androgen receptor activity altered ETS1 expression, which in turn altered the castrate-resistant phenotype. These data suggest a role for oncogenic ETS1 transcriptional activity in promoting aggressive prostate cancer and the castrate-resistant phenotype.

Introduction

Prostate cancer is the most commonly diagnosed cancer and the second leading cause of cancer death among men in the western world (1). Despite issues with overdiagnosis, prostate-specific antigen (PSA) screening has improved early detection methods and has led to the identification of thousands of men with localized prostate cancer that can be treated by prostatectomy and/or radiation treatment (2,3). However, there is a growing acceptance of initial active surveillance as opposed to definitive therapy in men with localized prostate cancer. This is because many men with prostate cancer have asymptomatic indolent disease that does not require immediate treatment (3). The optimum criteria for the identification of such men remain to be defined. However, a substantial number of patients treated for localized disease progress to an advanced stage or are already at an advanced stage at time of diagnosis (4,5). Advanced disease accounts

Abbreviations: ADT, androgen deprivation therapy; AKT, v-akt murine thymoma viral oncogene homolog; AR, androgen receptor; CRPC, castrate-resistant prostate cancer; ETS, v-ets erythroblastosis virus E26 oncogene; IHC, immunohistochemical studies; LNCaP, lymph-node carcinoma of the prostate; MAPK, mitogen-activated protein kinase; mRNA, messenger RNA; MUSC, Medical University of South Carolina; PSA, prostate-specific antigen; shRNA, short hairpin RNA; siRNA, small interfering RNA.

for the majority of prostate cancer-related deaths and is a result of lymphatic, local or contiguous spread. Androgen deprivation therapy (ADT) (medical castration, bilateral orchiectomy or both) targets androgen receptor (AR) activity by reducing available ligand (the hormone androgen) and is the standard of care for men with advanced prostate cancer (4,5). ADT decreases PSA levels, promotes tumor regression and improves patient symptoms (6). However, many patients undergoing ADT become resistant to its effects and progress to castrate (androgen/hormone)-resistant prostate cancer (CRPC). Despite the recent additions of several new agents, treatment strategies for patients with CRPC are inadequate, with progression-free survival rates as low as 2 months (6–8). The molecular events that augment the change from castrate-sensitive prostate cancer to CRPC are poorly understood but AR activity is thought to remain critical through the regulation of alternative gene sets to that observed in castrate-sensitive prostate cancer (9). Mechanisms mediating restoration of AR transcriptional activity in CRPC are thought to include (i) enhanced AR sensitivity to ligand; (ii) AR mutations which increase the AR ligand repertoire; (iii) activation by alternative signaling pathways; (iv) AR overexpression; (v) local tumor androgen production; (vi) intrinsic cell resistance and (vii) increased regulatory cofactor recruitment (10,11).

Mounting evidence associates members of the ETS (v-ets erythroblastosis virus E26 oncogene) family of transcription factors with prostate cancer progression as well as AR transcriptional activity (11). Whole-genome analysis in immortalized prostate cancer cells demonstrates that ∼70% of androgen response elements are adjacent to ETS consensus binding sites within gene promoters (12). AR–ETS transcriptional coregulation has been shown to regulate cancer-associated genes, such as members of the matrix metalloproteinase family (13,14), NKX3.1 (15), PTHrP (16), CCNG2 (12) and PSA (17). An analysis of over 14 000 molecular concepts identifies elevated ETS factor expression as a critical transition point at different stages of prostate cancer progression (18). Additionally, prostate cancer-specific chromosomal rearrangements between ETS family members (ERG, ETV1 and ETV4) and the androgen-responsive TMPRSS2 gene have been identified (19,20). In CRPC, ERG regulated trefoil 3 (TFF3) expression is a potential mechanism promoting tumor cell aggressiveness resulting from ERG rearrangements (21).

This study examines the contribution of the archetypical ETS factor ETS1 to prostate cancer progression and the castrate-resistant phenotype. ETS1 levels are increased in epithelial tumors, leukemia's, astrocytomas and sarcomas (22,23) and are increased in clinical and latent prostate cancer relative to benign prostatic hyperplasia and normal prostate (24). Thus, ETS1 represents a potential marker of poor prognosis (25–28). Increased ETS1 activity is associated with aberrant transcriptional regulation of multiple cancer-associated genes which can result in enhanced energy metabolism, cell survival, matrix degradation, cell growth, angiogenesis as well as migration and invasion (23,24,29). ETS1 activity has recently been associated with the castrate-resistant phenotype. Angiogenesis is increased in CRPC through increased levels of angiotensin II type-1 receptor expression (30,31). ETS1 is a direct regulator of angiotensin II and in castrate-resistant cells specifically, angiotensin II type-1 receptor therapeutic blockade inhibits angiogenesis through, at least in part, an inhibition of ETS1 expression (32).

This study demonstrates that ETS1 expression is highest in high-grade prostate cancer. *In vitro*, ETS1 expression and nuclear phosphorylation correlated with both aggression and the castrate-resistant phenotype in the lymph-node carcinoma of the prostate (LNCaP) model of prostate cancer progression. In the same model, elevated AKT (v-akt murine thymoma viral oncogene homolog) activity increased ETS1 protein levels preferentially in castrate-resistant cells and exogenous ETS1

expression rescued invasive potential when AKT activity was pharmacologically inhibited. Targeted AR activity altered ETS1 expression levels in immortalized cells. Significantly, modulated ETS1 expression altered the castrate-resistant response to AR antagonist treatment. In combination, these data strongly suggest a role for ETS1 transcriptional activity in promoting aggressive prostate cancer and the castrate-resistant phenotype.

Materials and methods

Tumor samples

Upon Institutional Review Board approval, RNA extracted from a cohort of 32 de-identified fresh frozen human prostate cancer tumor samples were obtained from the Hollings Cancer Center Tissue Biorepository here at the Medical University of South Carolina (MUSC). RNA concentration and integrity was monitored using an Agilent 2100 Bioanalyzer. Samples were divided into 16 low-grade (Gleason 4–6) and 16 high-grade (Gleason 7–9) groupings. Four normal prostate tissue samples were also obtained as controls. A subset of matching tissue samples were also obtained for immunohistochemical (IHC) studies. Prostate cancer tissue microarray slides containing 5× normal, 1× Gleason 3, 3× Gleason 4, 5× Gleason 5, 5× Gleason 6, 5× Gleason 7, 1× Gleason 8, 2× Gleason 9 and 2× Gleason 10 prostate tissue samples were obtained from US Biomax (Rockville, MD).

Cell culture

LNCaP prostate cancer progression cell lines consisting of the LNCaP parental line, LNCaP C4 (C4), LNCaP C4-2 (C4-2) and LNCaP C4-2B (C4-2B) were recently obtained from ViroMed (Minnetonka, MN) and cultured in the recommended media (33,34). Stocks were immediately generated and stored in liquid nitrogen. Cells were only cultured up to 30 passages before being replaced from low passage stocks. All cell lines were propagated at 37°C in an atmosphere containing 5% CO_2. Mycoplasma-negative cultures were ensured by PCR testing prior to investigations. Cells were monitored throughout for consistent morphology and doubling-time. Castrate-resistant LNCaP cells were developed by repeated passage in phenol red-free growth media containing 10% charcoal stripped fetal bovine serum (Invitrogen, Carlesbad, CA).

Immunohistochemistry

All tissue specimens obtained from the MUSC biorepository were formalin-fixed and paraffin-embedded. Samples/slides were rehydrated, and antigen retrieval was performed by heating in a vegetable steamer in 10 mM citrate, pH 6.0 for 30 min. Endogenous peroxidase activity was blocked using 0.3% H_2O_2 in methanol for 30 min. Sections were washed and non-specific binding was blocked using the VECTASTAIN Elite ABC kit (Vector Laboratories, Burlingame, CA) as instructed; then incubated overnight at 4°C with a target-specific primary antibody at a 1:100 dilution in the VECTASTAIN blocking solution. ETS1 primary antibody used for IHC was from Leica Biosystems (Chicago, IL). Overnight incubation at 4°C was followed by three 10 min washes in 1× Tris-buffered saline. Tissue staining was performed using the VECTASTAIN® Elite ABC peroxidase-based detection system and the Vector NovaRED substrate kit for peroxidase (Vector Laboratories) as per manufacturer's instructions. All sections were examined using an Olympus BX50 microscope and pictures were taken using an Olympus DP 70 camera connected to DP Controller software (Olympus, Center Valley, PA). Tissues were scored for intensity of staining and percent of specific staining of the cancer cells. The overall IHC score was calculated by multiplying the intensity score by the percent (%) of positive cells [IHC score = (intensity) × % positive cells] (35).

Real-time PCR analysis

One microgram of total RNA was reverse transcribed in a 20 µl reaction using iScript (Bio-Rad, Hercules, CA). Real-time PCR was performed with 5 µl of a 1:20 dilution of reverse transcribed complementary DNA using Roche SYBR Green qPCR master mix in a LightCycler480 (Roche, Nutley, NJ), as per the manufacturer's instructions. The cycling conditions for all genes were performed as per the manufacturer's recommendations: annealing temperature was 58°C. The size and purity of the PCR products were determined by melt curve analysis according to the Roche software. Primer sequences were: ETS1: forward—TCATTTCTTTGCTGCTTGGA, reverse—AAGCCGACTCTCAC-CATCAT; PSA: forward—GCAGCATTGAACCAGAGGAG, reverse—A-GAACTGGGGAGGCTTGAGT; AR: forward—CCTGGCTTCCGCAACTT ACAC, reverse—GGACTTGTGCATGCGGTACTCA; triplicate reactions were run for each complementary DNA sample. The relative expression of each gene was quantified on the basis of Ct value measured against an internal standard curve for each specific set of primers using the software provided by

the instrument manufacturer (Roche). After testing to define the optimal house-keeping gene (results not shown), tissue data were normalized to glyceraldehyde phosphate dehydrogenase (GAPDH) and cell line samples to S26 (GAPDH: forward—GAGTCAACGGATTTGGT, reverse—TTGATTTTGGAGGGATCT CG; S26: forward—GCGAGCGTCTTCGATGC, reverse—CTCAGCTCCTTA-CATGGGC).

Western blot analysis

LNCaP derived cell lines were used for isolation of total protein. Cells at 70–80% confluence were washed twice with ice-cold 1× phosphate-buffered saline and were lysed in RIPA buffer containing protease/phosphatase inhibitors (Sigma, St Louis, MO). Equal amounts of total protein (50 µg) were resolved by 10% sodium dodecyl sulfate–polyacrylamide gel electrophoresis and subjected to western blot analyses using Enhanced chemiluminescence system (Pierce–Fisher Scientific, Rockford, IL). Total protein lysates were examined for total ETS1 (C20; Santa Cruz, Santa Cruz, CA), ETS1^{pThr38} and ETS1$^{pSer282/285}$ (Invitrogen) and AR (N20;Santa Cruz). GAPDH was used as a loading control (Cell Signaling Technology, Danvers, MA).

Modulation of ETS1 and AKT expression

For transient ETS1 expression, 1 µg of pcDNA3-ETS1 construct containing the full ETS1 open reading frame (a kind gift from Dr Dennis Watson, Department of Pathology and Laboratory Medicine, MUSC) was transfected into LNCaP cells using Nanojuice transfection reagent (EMD, Gibbstown, NJ) and incubated in normal growth media for 48 h. Transient transfection of phosphorylation mutants of ETS1 (T38A and T38E—a kind gift from Dr Dennis Watson, MUSC) were also performed in the same manner. Stable pools of LNCaP cells expressing pcDNA-ETS1 were generated by repeated growth in media containing 300 µg/ml neomycin. To transiently reduce ETS1 expression, 50 nM of Stealth small interfering RNA (siRNA) primers specific for ETS1 or scrambled control (Qiagen, Valencia, CA) were transfected using Xtreme gene transfection reagent (Roche) and incubated in normal media for 48 h. C4-2-pooled cells stably expressing a short hairpin RNA (shRNA) vector, targeting ETS1 (pHUSH-ETS1; Origene, Rockville, MD), were generated by repeated selection in 1 µg/ml puromycin as per the vector manufacturer's instructions. For AKT1 exogenous expression, 1 µg of pBabe-AKT1 construct expressing myristoylated AKT (a kind gift from Dr Carola Neumann, Department of Pharmacology, MUSC) was also transfected using Nanojuice transfection reagent (EMD) as detailed above. Knockdown and overexpression levels were monitored by western blot analysis.

Transwell migration and invasion assays

Transiently transfected LNCaP cells expressing exogenous ETS1 or C4-2 cells, treated with ETS1-specific siRNA, were seeded in triplicate into the upper chamber of transwell inserts (BD Biosciences, San Diego, CA) either uncoated (for migration assessment) or precoated with matrigel (for invasion assessment) (Thermo Fisher Scientific, Hudson, NH) in serum-free media at a density of 100 000 cells per well. Media containing 10% serum was placed in the lower chamber to act as a chemoattractant, and cells were further incubated for 48 h. Control cells consisted of cells transiently transfected with control vector or scambled siRNA, respectively. Non-invasive cells were removed from the upper chamber by scraping and the cells remaining on the lower surface of the insert were stained using Diff-quick (Dade Behring, Newark, DE). Cells were quantified as the number of cells found in 10 random microscope fields. Error bars represent the standard deviation from three separate experiments.

Soft agar assay

Stable cells with exogenous or reduced ETS1 expression were used to analyze contact-independent growth. Two milliliters of 0.6% agarose in 2× Dulbecco's modified Eagle's medium were plated in each well of a six-well plate and left to set for 20 min. This layer was overlaid with 1.0×10^4 treated or control cells in 3 ml of 0.4% agarose diluted in 2× Dulbecco's modified Eagle's medium. Cells were incubated as normal for 14 days and the colonies were counted. Graphs represent the results from three experiments with three individual pooled stable clones.

Immunofluorescence

Cells were seeded onto sterile cover-slips (18 mm in diameter) coated with 5 µg/ml fibronectin and allowed to attach overnight. Cells were fixed with 2% formaldehyde, permeabilized with 0.1% Triton X-100 and blocked in 2% bovine serum albumin for 1 h at room temperature. Total ETS1 (unphosphorylated and phosphorylated), ETS1^{pThr38} and ETS1$^{pSer282/285}$ localization was examined using the antibodies detailed above and visualized using appropriate Alexa Fluor secondary antibodies (Invitrogen). TO-PRO was used as a nuclear stain (Invitrogen) and phalloidin (Invitrogen) was used to stain actin.

Immunofluorescence was examined using an Olympus IX70 confocal microscope and accompanying software.

Pharmacological treatment

Cells were seeded 50 000 in each well of a six-well plate and allowed to attach overnight. The following day, cells were treated with 1 nM R1881 (Perkin Elmer, San Jose, CA), 10 μM LY294002 or 10 μM U0126 (Cell Signaling Technology), respectively. Cells were incubated for 24 h before collection and analysis.

Co-immunoprecipitation assays

ETS1–AR protein interaction was investigated using Invitrogen's Dynabead Co-IP kit as per instructions using Dynabead cross-linked C20 ETS1 antibody for immunoprecipitation and N20 AR antibody for western blot (Santa Cruz).

Cell viability assays

Stable cells with exogenous or reduced ETS1 expression were used for analysis in cell viability assays. Cells were trypsinized and 50 000 seeded into individual wells on a six-well plate and allowed to attach overnight. Cells were treated with 10 nM Flutamide (Sigma) for 72 h. Drug was replaced every 24 h after which cell growth medium was isolated to collect dead and unattached cells and the attached cells trypsinized and combined with the growth medium. The combined cell lysate was then centrifuged at 2500 r.p.m. to collect the cell pellet containing both dead and viable cells. Cells were resuspended in 250 μl of 1× phosphate-buffered saline and 10 μl was stained with trypan blue and loaded onto a counting chamber. Dead and viable cells were quantified in triplicate using a Countess Cell Counter (Invitrogen). Graphs represent the results from three experiments with three individual pooled stable clones.

Statistical analysis

For statistical testing, two-sample unpaired Student's t-tests were calculated. In general, $P < 0.05$ was considered statistically significant. Error bars represent standard deviations of independent experiments unless indicated otherwise.

Results

ETS1 levels are elevated in high-grade human prostate cancer tissues

Human prostate cancer tissue samples were divided into 16 low-grade (Gleason 5 and 6) and 16 high-grade (Gleason 7–9) groups. Four normal prostate samples were also analyzed as controls. Reverse transcription–PCR analysis shows a significant increase in ETS1 messenger RNA (mRNA) levels in high Gleason grade tumors compared with low Gleason grade (Figure 1A and B). Similar ETS1 expression levels were observed for normal prostate and low Gleason grade tumors and elevated ETS1 protein levels in high-grade tumors were confirmed in a subset of corresponding tumor samples by IHC (Supplementary Figure 1 is available at *Carcinogenesis* Online). ETS1 protein expression levels were also analyzed by tissue microarray analysis and confirmed increased ETS1 expression in high-grade prostate cancer (Figure 1C). Compared with normal prostate, no statistical difference in ETS1 staining was observed in Gleason 3, 4 or 5 tumor samples (Figure 1C and D). However, a statistically significant increase in ETS1 staining intensity was observed in high-grade tumor samples of Gleason 7 (4/5), 9 (1/2) and 10 (2/2) (Figure 1C) but not in the single grade 8 tumor sample on the slide (Figure 1C). When present, positive ETS1 staining in normal and low-grade tumor samples (Gleason 3–6) was mainly confined to the stromal compartment but was predominantly nuclear in the higher grade samples (see insets Figure 1D).

Increased ETS1 levels correlate with aggression and castrate resistance in the LNCaP progression model

The four cell lines comprising Leland Chung's LNCaP progression model reflect increasing invasive/metastatic ability and the castrate-sensitive (LNCaP) and castrate-resistant (C4, C4-2 and C4-2B) phenotypes (33,34). To establish an *in vitro* model for examining ETS1 function, ETS1 mRNA and protein levels were examined in all four cell lines by real-time PCR and western blot analysis, respectively. Increasing PSA mRNA levels (Figure 2A) and slightly reduced AR protein levels (Figure 2B) are characteristics for this progression model (36). ETS1 mRNA levels were elevated in all three derivative cell lines compared with LNCaP. Highest mRNA levels were observed in the C4 cell line (Figure 2A) but this was not reflected

at the protein level. However, we observed a moderate but robust increase in ETS1 protein expression in the two most aggressive castrate-resistant cell lines (1.7-fold in C4-2 and 2.8-fold in C4-2B) compared with the LNCaP parental (Figure 2B).

To assess the contribution of ETS1 activity to the aggressive phenotype, we examined the effect of targeting ETS1 expression in the LNCaP parental and C4-2 subline. ETS1 was exogenously expressed in LNCaP cells transfected with pcDNA3-ETS1 vector (Figure 2C, left) and ETS1 levels reduced in C4-2 cells transiently transfected with siRNA (Figure 2C, middle) or stably transfected with shRNA vector (Figure 2C, right) targeting ETS1. Compared with controls, we observed an ∼12-fold increase and ∼8-fold decrease in ETS1 expression 48 h post-transfection (Figure 2C). In transwell invasion assays through matrigel-coated inserts, exogenous ETS1 expression in the LNCaP parental line increased invasive capacity to levels comparable with the more invasive C4-2 subline (Figure 2D). siRNA targeting of ETS1 expression in C4-2 reciprocally reduced invasive capacity to levels similar to that observed for parental LNCaP cells (Figure 2D). Although modulated ETS1 expression does affect cell viability at the 72 h time-point (as shown in Figure 6), this was statistically insignificant at the 48 h time-point used in the invasion assays (results not shown).

Although cells cannot invade without motile function, conformation of the ability of ETS1 to stimulate cellular migration was confirmed in Transwell migration assays (Supplementary Figure 2A is available at *Carcinogenesis* Online). Once again increased ETS1 expression promoted and loss of ETS1 expression inhibited the migratory ability of LNCaP and C4-2 cells, respectively. C4 cells did not demonstrate increased ETS1 protein levels compared with the parental LNCaP cell line. However, siRNA-mediated ETS1 loss in these cells still inhibited invasive potential (Supplementary Figure 2B is available at *Carcinogenesis* Online). Similar effects were observed in soft agar assays, where stable ETS1 expression in LNCaP cells increased anchorage-independent growth to C4-2 levels and stable ETS1 loss (shRNA) decreased anchorage-independent growth closer to LNCaP levels (Figure 2E; Supplementary Figure 3 is available at *Carcinogenesis* Online).

Activating ETS1 phosphorylation increases with progression in the LNCaP prostate cancer model

ETS1 transcriptional activity is regulated by post-translational modification (37–39), so we examined the phosphorylation status of ETS1 in the LNCaP progression model. Immunofluorescence studies in the castrate-sensitive LNCaP (Figure 3A) and castrate-resistant C4-2 (Figure 3B) cell lines demonstrates cytoplasmic and nuclear staining for total ETS1. An examination of phosphorylated ETS1 localization using ETS1^{pThr38}- and ETS1$^{pSer282/285}$-specific antibodies shows only nuclear staining in both the LNCaP and C4-2 cell lines. Furthermore, a comparison of phosphorylated protein levels by western blot analysis defines a graduated increase in ETS1^{pThr38} through the LNCaP, C4, C4-2 and C4-2B cell lines and a graduated decrease in ETS1$^{pSer282/285}$ (Figure 3C). This indicates increased ETS1 transcriptional activity (37,38) in the more aggressive castrate-resistant cell lines. As ETS1 protein expression levels are not elevated in the C4 cell line compared with LNCaP parental cells (Figure 2B), these results indicate that increased ETS1 transcriptional activation rather than increased expression may promote its oncogenic activity in this least invasive castrate-resistant cell line.

ETS1^{Thr38} phosphorylation is mediated by the mitogen-activated protein kinase (MAPK)–extracellular signal-regulated kinase pathway (38,40,41). To examine if this pathway inhibits ETS1 function, MAPK activity was pharmacologically inhibited in C4-2 cells using the MAPK kinase inhibitor U0126 (10 μM for 24 h) and invasive potential examined in transwell invasion assays. As observed for LNCaP parental cells (Figure 2E), exogenous expression of ETS1 in the C4-2 derivative increased invasive potential (Figure 3D). Inhibition of MAPK activity with U0126 reduced the ability of C4-2 cells to invade across matrigel-coated membranes but invasive potential was partially restored
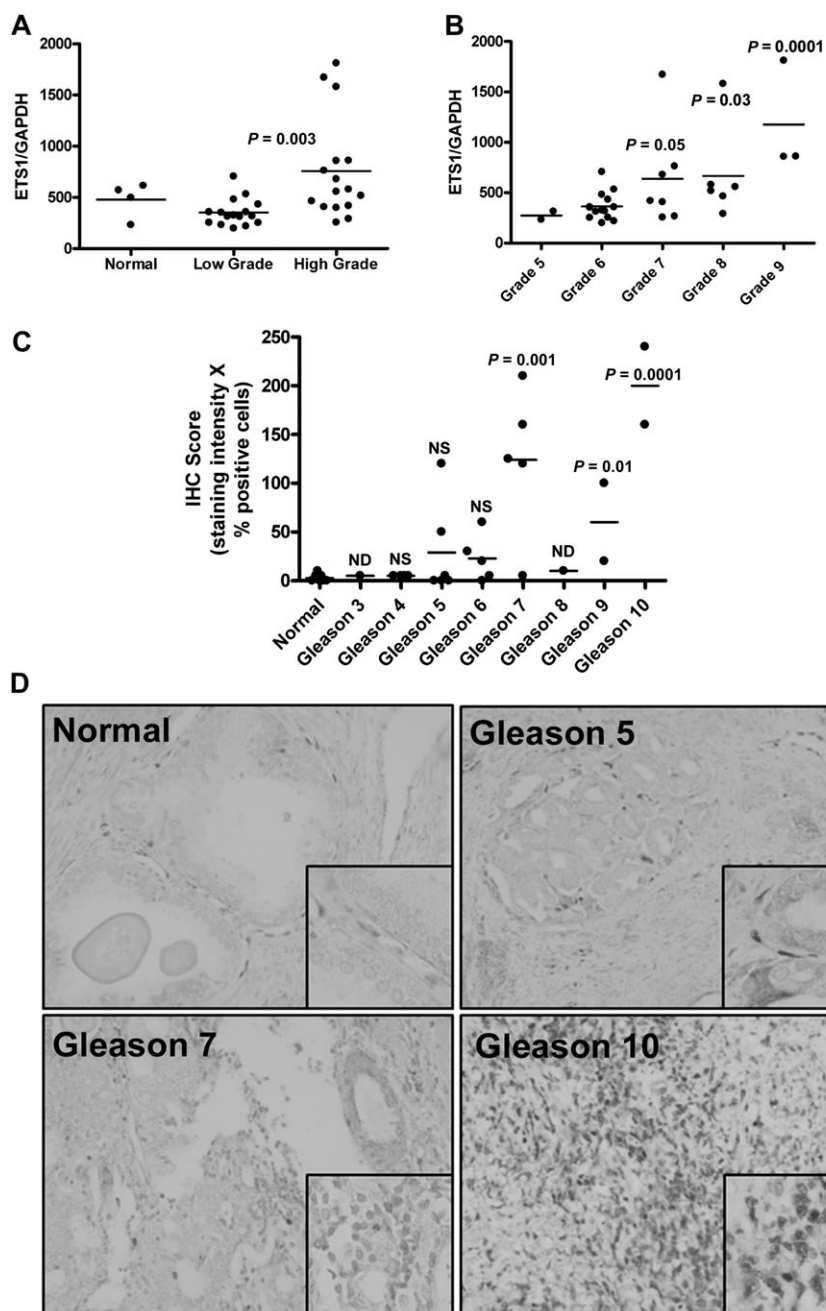
Fig. 1. ETS1 levels are elevated in high-grade human prostate cancer tissues and correlate with high PSA. (**A**) Real-time PCR analysis of ETS1 mRNA levels in a cohort of 16 low-grade (Gleason 5 and 6) and high-grade (Gleason 7–9) human prostate cancer samples. *P* values calculated relative to normal prostate values. (**B**) Real-time PCR analysis of ETS1 mRNA extrapolated to show individual Gleason score levels of ETS1 mRNA expression. *P* values calculated relative to Gleason 6 values. (**C**) Tissue microarray analysis of ETS1 protein expression in normal and prostate cancer tissue samples. *P* values calculated relative to normal prostate values. NS, not significant; ND, not determined. (**D**) Representative IHC staining of ETS1 protein levels on the tissue microarray. Large pictures ×20 and insets ×40 magnification.

when ETS1 was exogenously expressed in U0126-treated cells (Figure 3D). The effect of exogenous expression of ETS1 phosphorylation mutants on invasive potential was also examined. Compared with the endogenous expression of wild-type ETS1, expression of constitutively active ETS1 (T38E) stimulated invasive potential of LNCaP cells, whereas expression of a phosphorylation inactive ETS1 mutant (T38A) did not stimulate invasive potential (Figure 3E).

The AKT pathway stimulates ETS1 expression in castrate-resistant cells

The AKT signaling pathway is implicated in prostate cancer progression and the castrate-resistant phenotype (42,43). We examined a possible relationship between AKT activity and increased ETS1 levels in the LNCaP prostate cancer model. We observed an increase in AKT activity within the LNCaP progression model as represented by increased AKT phosphorylation at Ser 473 (Figure 4A), which is known to correlate with increased aggression and the castrate-resistant phenotype (31,44). We next examined the effect of modulated AKT activity on ETS1 protein expression and biological function. Pharmacological inhibition of phosphorylated AKT with the PI3K inhibitor LY294002 (10 μM or 20 μM for 24 h) reduced ETS1 protein levels in castrate-resistant C4-2 cells but not to the same extent in castrate-sensitive LNCaP cells (Figure 4B). As shown by western blot analysis, exogenous expression of constitutively activated

575
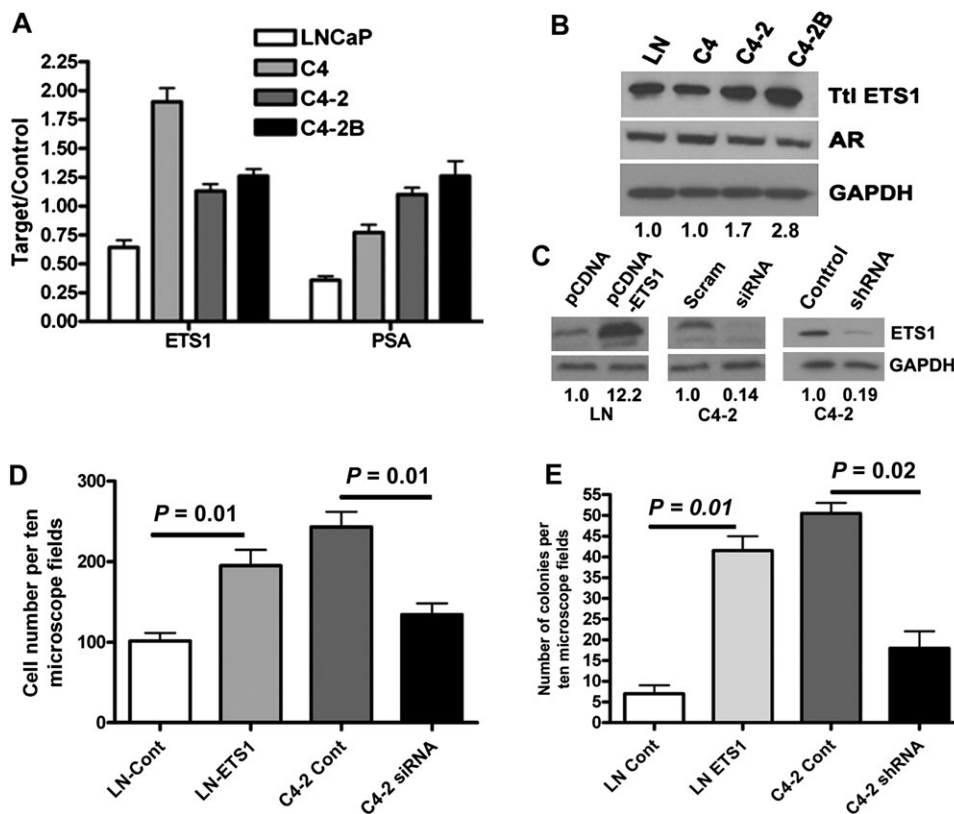
Fig. 2. Increased ETS1 levels correlate with aggression and castrate resistance in the LNCaP progression model. (**A**) Real-time PCR analysis of ETS1 and PSA mRNA levels in the LNCaP cell line model of prostate cancer progression. All data was normalized to S26 levels. (**B**) Western blot showing ETS1 and AR protein levels in the LNCaP cell line model of prostate cancer progression. GAPDH levels are shown as a loading control. Numbers represent fold difference in expression compared with LNCaP (LN). (**C**) Western blot showing levels of ETS1 expression after (1) transfection with control (pcDNA) and pcDNA-ETS1 expression vector in LNCaP cells (left panel), (2) transient transfection with scrambled (scram) and ETS1-targeting siRNA (siRNA) in C4-2 cells (middle panel) and (3) stable expression of a short hairpin vector targeting ETS1 (shRNA) or control vector. GAPDH levels are shown as a loading control. Numbers represent fold difference in expression. (**D**) Transwell invasion assay examining the effect of transient ETS1 expression in LNCaP prostate cancer cells transfected with pcDNA (LN-Cont) or pcDNA-ETS1 (LN-ETS1) and reduced expression of ETS1 in C4-2 prostate cancer cells transfected with scrambled control (C4-2 Cont) or siRNA targeting ETS1 (C4-2 siRNA). Error bars represent the standard deviation from three separate experiments. (**E**) Soft agar assay examining the effect of stable ETS1 expression in LNCaP prostate cancer cells transfected with pcDNA (LN-Cont) or pcDNA-ETS1 (LN-ETS1) and reduced expression of ETS1 in C4-2 prostate cancer cells stably transfected with control (C4-2 Cont) or shRNA vector targeting ETS1 (C4-2 shRNA). Graphs represent the results from three experiments with three individual pooled stable clones.

(myristoylated) AKT1 in LNCaP cells leads to a significant increase in ETS1 protein levels (Figure 4C). Once again exogenous expression of ETS1 in the C4-2 derivative subline increased invasive potential in transwell invasion assays (Figure 4D). Inhibition of AKT activity with LY294002 reduced the ability of C4-2 cells to invade across matrigel-coated membranes but invasive potential was restored when ETS1 was exogenously expressed in LY294002-treated cells (Figure 4D). Exogenous expression of AKT was also sufficient to rescue invasive potential in the presence of LY294002 (Supplementary Figure 4 is available at *Carcinogenesis* Online).

Targeted AR activity alters ETS1 expression levels

When castrate-sensitive prostate cancer cells are grown in hormone-depleted (phenol red free and charcoal stripped) media, AR activity is inhibited by the reduction of receptor ligand, which induces cell growth inhibition and apoptosis. We examined the effect of AR ligand deprivation on ETS1 protein expression in castrate-sensitive LNCaP cells and found a significant reduction in ETS1 protein levels after 7 days of growth in hormone-deprived media (Figure 5A). Prolonged culture of LNCaP cells in hormone-depleted media (eight passages and above) produces a castrate-resistant subline (castrate-resistant LNCaP cells). An examination of ETS1 protein levels in castrate-resistant LNCaP cells shows a significant restoration of ETS1 expression upon the loss of androgen dependence and acquisition of castrate resistance (Figure 5B). R1881 is a synthetic androgen,

which stimulates AR transcriptional activation to promote cell proliferation and tumor growth *in vitro* and *in vivo*. Treatment of LNCaP cells with R1881 (1 nM for 24 h) produces a substantial increase in ETS1 protein expression as shown by western blot analysis (Figure 5C). To investigate the potential ETS1–AR interaction further, we performed co-immunoprecipitation analysis to pull down ETS1–AR complexes in the LNCaP-derived cell lines. Although AR levels are slightly reduced in the C4-2 and C4-2B cells (Figure 2B), we observed an increase in ETS1–AR protein–protein interaction in these two LNCaP castrate-resistant derivatives compared with the parental castrate-sensitive LNCaP line (Figure 5D).

Modulated ETS1 alters sensitivity to AR antagonist in castrate-resistant cells

To examine the effects of ETS1 expression on the castrate-resistant phenotype, we used ETS1 gain-of-function and loss-of-function studies in the LNCaP and C4-2 cell lines, respectively. Cell viability assays analyzed using a Countess Automated Cell Counter (Invitrogen) after cell trypan blue staining were used to assess the effect of Flutamide treatment on LNCaP cells with exogenous ETS1 expression and C4-2 cells with reduced ETS1 expression. Exogenous ETS1 levels were induced by stable transfection with a pCDNA3 expression vector containing the ETS1 open reading frame (Figure 2C, left) and ETS1 levels were reduced by stable expression of shRNA targeting ETS1 (Figure 2C, right). Exogenous
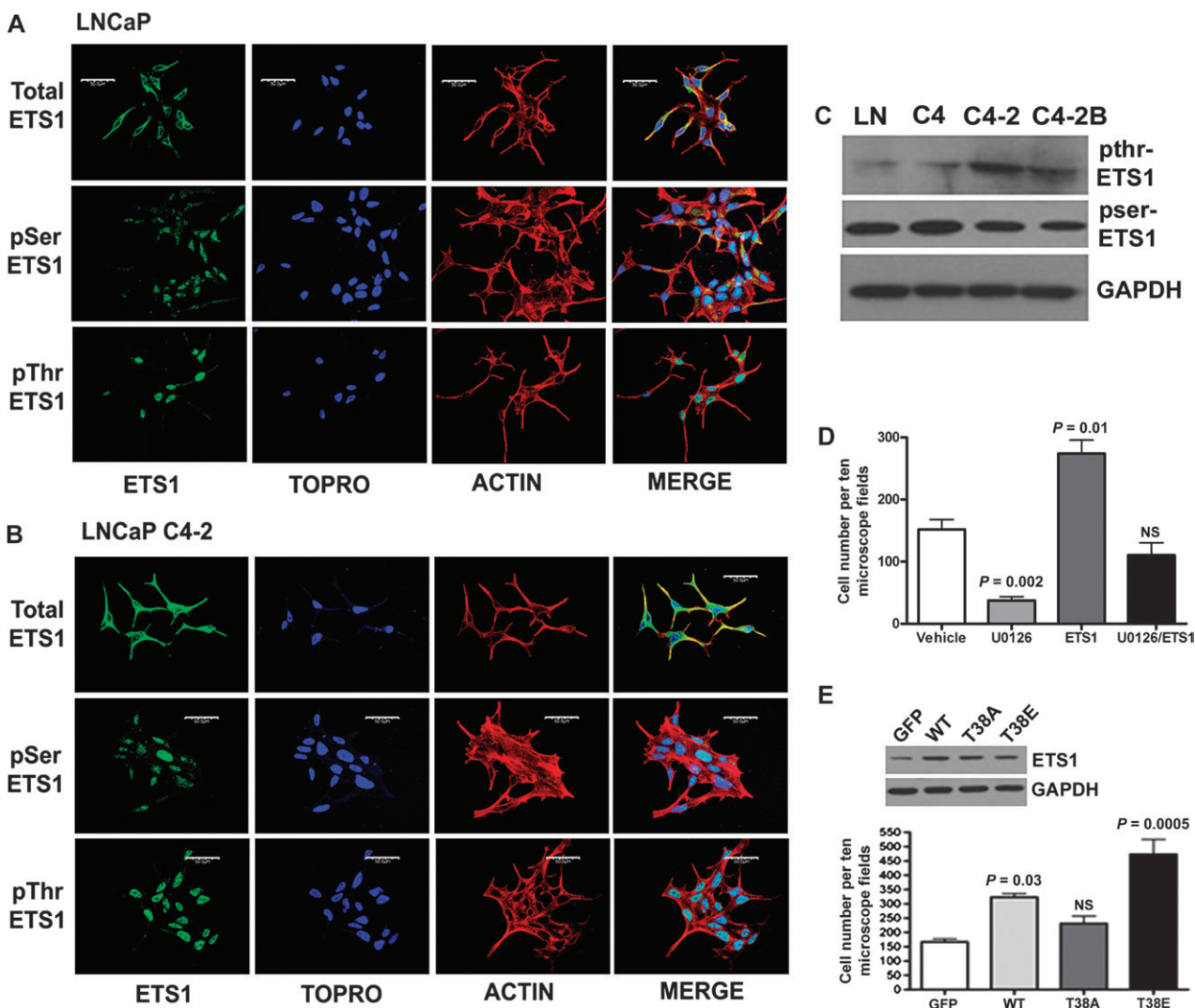
Fig. 3. Activating ETS1 phosphorylation increases with progression in the LNCaP prostate cancer model. (**A** and **B**). Immunofluorescent analysis of total ETS1 (unphosphorylated and phosphorylated), ETS1Thr38 (pThr ETS1) and ETS1pSer282/285 (pSer ETS1) protein expression and localization in LNCaP (A) and C4-2 (B) immortalized prostate cancer cells (green). TO-PRO was used as a nuclear stain (blue) and phalloidin was used to stain actin (red). A merged image is also shown. (**C**) Western blot showing ETS1pThr38 and ETS1pSer282/285 protein levels in the LNCaP prostate cancer progression model. GAPDH is shown as a loading control. (**D**) Transwell invasion assay comparing the effects of MEK inhibitor treatment (10 μM U0126 for 24 h) in the presence and absence of exogenous ETS1 expression on invasive potential in C4-2 prostate cancer cells. Error bars represent the standard deviation from three separate experiments. NS, not significant. (**E**) Transwell invasion assay examining the effects of ETS1 phosphorylation mutants (T38A and T38E) on invasive potential compared with LNCaP wild-type control. Error bars represent the standard deviation from three separate experiments. Comparative ETS1 protein expression levels for each of the constructs are shown above. NS, not significant.

ETS1 expression promoted proliferation in LNCaP cells in the absence of drug compared with vehicle-only controls (Figure 6A). Treatment of the same cells with 10 nM Flutamide for 72 h (Figure 6A), significantly inhibited proliferation and increased the number of trypan blue-positive (apoptotic) cells. However, in LNCaP cells with elevated ETS1 levels, proliferation was significantly rescued and the fraction of apoptotic cells was reduced after Flutamide treatment, indicating that ETS1 expression conferred a castrate-resistant phenotype to LNCaP cells (Figure 6A). Reduced ETS1 expression in the absence of Flutamide significantly reduced the proliferative capacity of castrate-resistant C4-2 cells and also induced apoptosis compared with vehicle-only controls (Figure 6B). Treatment of C4-2 cells with 10 nM Flutamide (72 h) showed only a small inhibition of proliferation and no evidence of apoptosis was observed (Figure 6B). However when ETS1 levels were reduced in combination with Flutamide treatment, proliferation was significantly reduced over that observed when ETS1 levels only were reduced and a significant fraction of apoptotic cells was observed (Figure 6B). This indicates that loss of ETS1 expression may restore sensitivity to AR antagonist treatment in the castrate-resistant background.

Discussion

For men with newly diagnosed localized prostate cancer, the decision whether to pursue active surveillance or definitive therapy ('to treat or not to treat') continues to be a challenge. Therefore, more accurate and reliable predictive biomarkers are urgently needed to be able to distinguish patients with indolent slow-growing tumors who may be more appropriate for active surveillance from patients with potentially lethal tumors, requiring definitive treatment (surgery or radiation therapy). Through the dysregulation of its transcriptional target genes, increased ETS1 activity provides a mechanism, which can promote multiple cancer-associated pathways. This study demonstrates that increased ETS1 expression correlates with prostate tumors of Gleason 7 and above. Gleason 7 tumors represent a critical point in the aggressive phenotype of prostate cancer. Disease-specific survival is 10
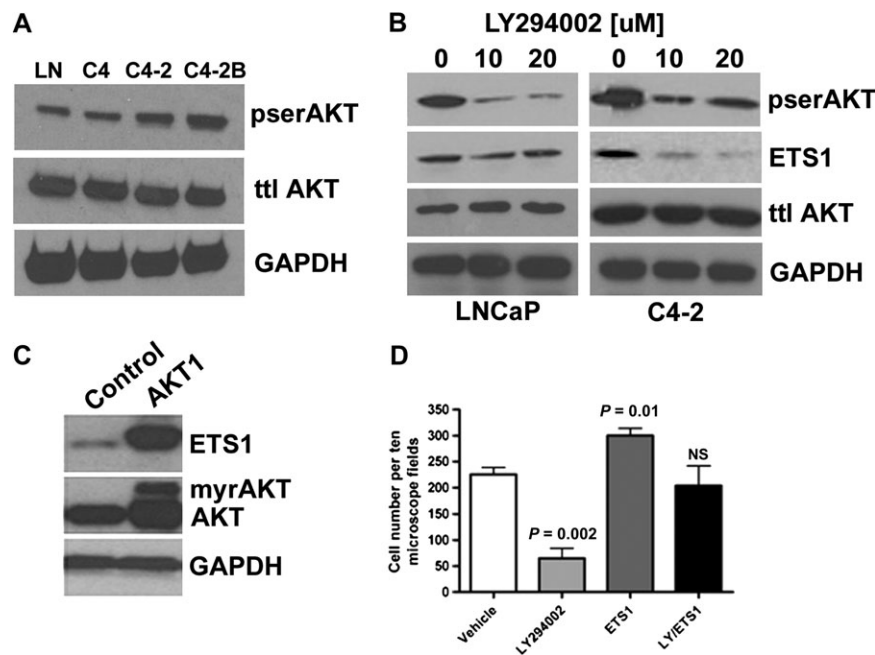
Fig. 4. The AKT pathway stimulates ETS1 expression in castrate-resistant cells. (**A**) Western blot showing phosphorylated (pserAKT) and total AKT (ttl AKT) expression in the LNCaP prostate cancer progression model. GAPDH is shown as a loading control. (**B**) Western blot analysis of ETS1, phosphorylated and total AKT expression after treatment with PI3K inhibitor (10 µM and 20 µM LY294002 for 24 h). GAPDH is shown as a loading control. (**C**) Western blot showing levels of ETS1 and AKT expression after transfection with pBabe empty vector (control) and pBabe-AKT (myrAKT) expression vector (AKT1) in LNCaP cells. GAPDH is shown as a loading control. (**D**) Transwell invasion assay comparing the effects of PI3K inhibitor treatment (10 µM LY294002 for 24 h) in the presence and absence of exogenous ETS1 expression on invasive potential in C4-2 prostate cancer cells. Error bars represent the standard deviation from three separate experiments. NS, not significant.
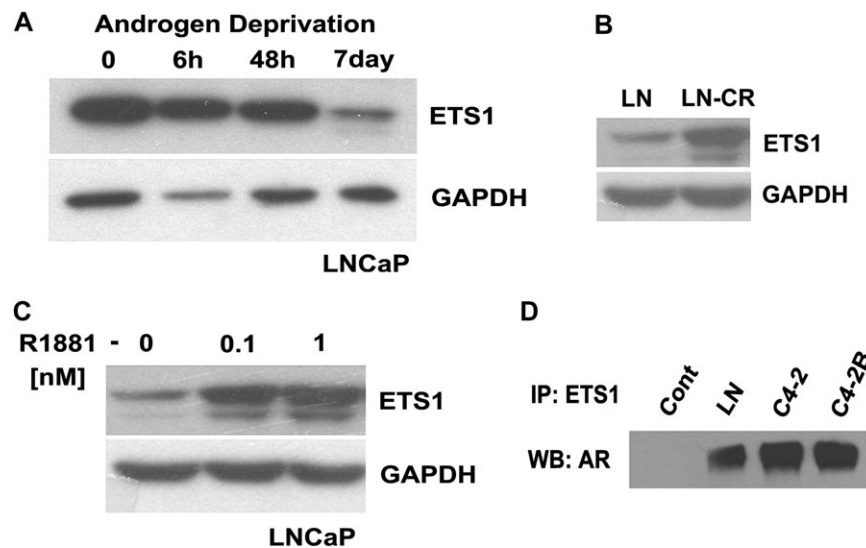

Fig. 5. Targeted AR activity alters ETS1 expression levels. (**A**) Western blot showing ETS1 expression levels in LNCaP prostate cancer cells after culture in androgen-deprived media for the indicated time points. GAPDH is shown as a loading control. (**B**) Western blot showing ETS1 expression levels in LNCaP (LN) and castrate-resistant LNCaP prostate cancer cells. GAPDH is shown as a loading control. (**C**) Western blot showing ETS1 expression levels in LNCaP prostate cancer cells after treatment with the AR agonist R1881 (0–1 nM for 24 h). GAPDH is shown as a loading control. (**D**) Co-immunoprecipitation (IP) analysis of ETS1–AR protein–protein complexes in the LNCaP prostate cancer progression model.

years for Gleason 7 but 16 years for Gleason 6. Mean tumor volume is 5.1 cc's for Gleason 7 compared with ∼2.5 cc's for Gleason 5 and 6 and there is a 10-fold increase in the risk of positive lymph nodes and/or seminal vesicles in Gleason 7 patients (45). Further analysis is warranted in a larger cohort of patients with detailed treatment and outcome data to fully investigate if higher ETS1 expression in lower grade tumor samples is indicative of poor outcome and represents a potential biomarker for prostate cancer progression. If this is the case, ETS1 expression levels may help identify those patients with

potentially aggressive tumors requiring more stringent therapy from those with slow-growing tumors who would benefit from a 'watch and wait' treatment strategy.

Using the LNCaP prostate cancer model, mechanistic insight was gained into the regulatory pathways controlling ETS1 transcriptional activity during prostate cancer progression to the castrate-resistant phenotype. The LNCaP model represents increasingly aggressive prostate cancer and the transition from a castrate-sensitive (LNCaP) to a castrate-resistant phenotype (C4, C4-2 and C4-2B) (33,34). The

A

LNCaP ETS1 O/E

B

LNCaP C4-2 shETS1
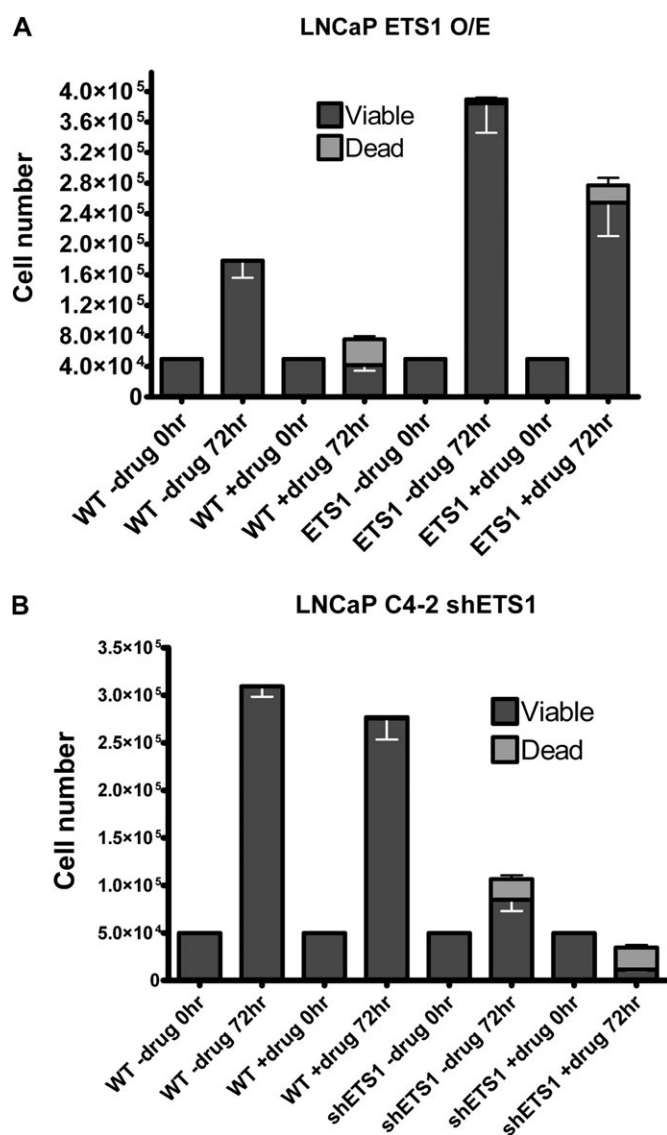
Fig. 6. Modulated ETS1 alters sensitivity to AR antagonist in castrate-resistant cells. (**A**) Cell viability assays comparing the effects of exogenous ETS1 expression on the response to 10 μM Flutamide treatment (+drug) for 72 h in LNCaP prostate cancer cells stably expressing ETS1 (ETS1) or vector control (WT, wild-type). (**B**) Cell viability assays comparing the effects of reduced ETS1 expression on the response to 10 μM Flutamide treatment (+drug) for 72 h in C4-2 prostate cancer cells stably expressing a short hairpin vector against ETS1 (shETS1) or vector control (WT, wild-type).

parental LNCaP line does not form tumors in mice without the presence of matrigel and although the C4 subline forms tumors in intact mice, it does not readily form tumors in castrated mice (36). The highly aggressive C4-2 and C4-2B sublines however form tumors in both intact and castrated mice and C4-2B readily metastasizes to the bone (36).

In this study, increased ETS1 expression and transcriptional activity was identified as a possible mechanism promoting the aggressive phenotype of the castrate-resistant C4-2 and C4-2B LNCaP derivatives. Transcription factors, such as ETS1, have been identified as critical regulators of many normal and aberrant biological processes as they influence the expression of large groups of genes. As critical regulators, relatively small increases or decreases in their expression can alter critical gene regulatory networks to direct cell fate. Additionally, the increased expression of a transcription factor is not a requirement for increased transcriptional activation at target gene promoters. For example, increased post-translational modification is a common mechanism increasing the magnitude of transcription

factor activity without a requirement for increased expression. Elevated ETS1 expression in our progression model was accompanied by an increase in the levels of nuclear transcriptionally active ETS1, as defined by increased Thr38 and decreased Ser282/285 phosphorylation. RAS–MAPK-mediated phosphorylation at threonine-38 increases ETS1 DNA-binding activity through, for example, the recruitment of CREB binding protein which stimulates ETS1 transcriptional activity (38–41). In contrast, CAMKII phosphorylation of ETS1 at a series of four serine residues adjacent to the ETS1 DNA-binding domain activates its autoinhibition loop to inhibit transcriptional activity (37). Further evidence suggests that ETS1 cofactor binding can function to override its autoinhibition (46) and together these molecular events function to regulate ETS1 DNA-binding ability and control its regulation of transcriptional target genes. In combination, these factors may be sufficient to have significant effects on downstream target gene expression and the biological pathways they control. This is supported by the fact that we observe no increase in ETS1 protein expression in less invasive C4 cells but do observe a 2-fold increase in ETS1 phosphorylation at Thr38, which is indicative of increased ETS1 transcriptional activation. Increased ETS1 transcriptional activity at the PSA promoter rather than increased ETS1 expression would also explain why ETS1 protein levels do not correlate with PSA in the C4 cell line.

Interestingly, MAPK activation can increase the levels of AR-dependent gene sets in the absence of androgens through direct AR phosphorylation and/or through phosphorylation of other transcription cofactors and can also stimulate prostate cancer growth independently of AR (47–50). In CRPC, activated MAPK levels can stimulate the growth of prostate cancer cells through the activation of alternative transcription factors to AR, such as AP1 and c-myc (47,50–52). Coordinate and individual activation of the MAPK and AKT signaling pathways have been demonstrated in advanced prostate cancer and combinatorial targeting of these two pathways inhibits the castrate-resistant phenotype in preclinical mouse studies (53). AKT is a downstream effecter of the PI3K pathway. Its increased activation has been shown to be a potential indicator of poor prognosis in prostate cancer (54) and mediator of the castrate-resistant phenotype in mouse models and immortalized cell lines (42,43).

Although ADT is the standard of care for men with advanced prostate cancer (4,5), most patients eventually progress to a castration resistant state, and treatments for CRPC are not optimal (6–8). There is a need for a greater understanding of the molecular mechanism promoting the castrate-resistant phenotype so that effective therapeutic regimes can be developed. Improved understanding of the pathology of prostate cancer before and after ADT could lead to better predictors of treatment response and outcomes. Combinatorial control is a critical factor in ETS1-mediated transcriptional regulation through synergistic interactions with other key transcription factors at composite consensus sites (11). Around 70% of ETS-binding sites are adjacent to AR response elements (12). ETS1 expression, activation status and molecular complexes with AR are increased in the more aggressive and castrate-resistant sublines. These studies also demonstrate that modulated ETS1 expression can alter the castrate-resistant phenotype. Although ETS1 activity may decrease as an initial response to hormone deprivation, LNCaP cells are able to adapt to the depleted environment and restore ETS1 activity possibly to promote the castrate-resistant phenotype. Significantly, increased ETS1 activity promoted resistance to treatment with the AR antagonist Flutamide, whereas loss of ETS1 function restored sensitivity. These data suggest that there may be benefit to targeting ETS1 in patients with CRPC. It is tempting to hypothesize that ETS1 expression and transcriptional activity is increased possibly through the AKT and MAPK signaling pathways to enhance ETS1 aberrant gene regulation to promote the castrate-resistant phenotype. Further analysis is required to fully define the role of ETS1 to castrate resistance and identify if these ETS1-mediated effects are AR dependent, independent or both.

Supplementary material

Supplementary Figures 1–4 can be found at http://carcin.oxford journals.org/.

References

1. Jemal,A. *et al.* (2008) Cancer statistics, 2008. *CA Cancer J. Clin.*, **58**, 71–96.
2. Schroder,F.H. *et al.* (2009) Screening and prostate-cancer mortality in a randomized European study. *N. Engl. J. Med.*, **360**, 1320–1328.
3. Bangma,C.H. *et al.* (2007) Overdiagnosis and overtreatment of early detected prostate cancer. *World J. Urol.*, **25**, 3–9.
4. Heidenreich,A. *et al.* (2009) [EAU guidelines on prostate cancer]. *Actas Urol. Esp.*, **33**, 113–126.
5. Heidenreich,A. *et al.* (2008) EAU guidelines on prostate cancer. *Eur. Urol.*, **53**, 68–80.
6. Loblaw,D.A. *et al.* (2007) Initial hormonal management of androgen-sensitive metastatic, recurrent, or progressive prostate cancer: 2006 update of an American Society of Clinical Oncology practice guideline. *J. Clin. Oncol.*, **25**, 1596–1605.
7. Chang,S.S. (2007) Treatment options for hormone-refractory prostate cancer. *Rev. Urol.*, **9** (suppl. 2), S13–S18.
8. Kish,J.A. *et al.* (2001) The treatment challenge of hormone-refractory prostate cancer. *Cancer Control*, **8**, 487–495.
9. Wang,Q. *et al.* (2009) Androgen receptor regulates a distinct transcription program in androgen-independent prostate cancer. *Cell*, **138**, 245–256.
10. Chen,C.D. *et al.* (2004) Molecular determinants of resistance to antiandrogen therapy. *Nat. Med.*, **10**, 33–39.
11. Turner,D.P. (2010) The role of ETS transcriptional regulation in hormone sensitive and refractory prostate cancer. *Open Cancer J.*, **3**, 40–48.
12. Massie,C.E. *et al.* (2007) New androgen receptor genomic targets show an interaction with the ETS1 transcription factor. *EMBO Rep.*, **8**, 871–878.
13. Schneikert,J. *et al.* (1996) Androgen receptor-Ets protein interaction is a novel mechanism for steroid hormone-mediated down-modulation of matrix metalloproteinase expression. *J. Biol. Chem.*, **271**, 23907–23913.
14. Singh,S. *et al.* (2002) ETS proteins and MMPs: partners in invasion and metastasis. *Curr. Drug Targets*, **3**, 359–367.
15. Preece,D.M. *et al.* (2011) ETS1 regulates NKX3.1 5' promoter activity and expression in prostate cancer cells. *Prostate*, **71**, 403–414.
16. Asadi,F. *et al.* (2005) Parathyroid hormone-related protein in prostate cancer. *Crit. Rev. Eukaryot. Gene Expr.*, **15**, 15–28.
17. Chen,H. *et al.* (2002) NKX-3.1 interacts with prostate-derived Ets factor and regulates the activity of the PSA promoter. *Cancer Res.*, **62**, 338–340.
18. Tomlins,S.A. *et al.* (2007) Integrative molecular concept modeling of prostate cancer progression. *Nat. Genet.*, **39**, 41–51.
19. Tomlins,S.A. *et al.* (2009) ETS gene fusions in prostate cancer: from discovery to daily clinical practice. *Eur. Urol.*, **56**, 275–286.
20. Attard,G. *et al.* (2009) Hormone-sensitive prostate cancer: a case of ETS gene fusion heterogeneity. *J. Clin. Pathol.*, **62**, 373–376.
21. Rickman,D.S. *et al.* (2010) ERG cooperates with androgen receptor in regulating trefoil factor 3 in prostate cancer disease progression. *Neoplasia*, **12**, 1031–1040.
22. Seth,A. *et al.* (2005) ETS transcription factors and their emerging roles in human cancer. *Eur. J. Cancer*, **41**, 2462–2478.
23. Turner,D.P. *et al.* (2008) ETS transcription factors: oncogenes and tumor suppressor genes as therapeutic targets for prostate cancer. *Expert Rev. Anticancer Ther.*, **8**, 33–42.
24. Alipov,G. *et al.* (2005) Overexpression of Ets-1 proto-oncogene in latent and clinical prostatic carcinomas. *Histopathology*, **46**, 202–208.
25. Span,P.N. *et al.* (2002) Expression of the transcription factor Ets-1 is an independent prognostic marker for relapse-free survival in breast cancer. *Oncogene*, **21**, 8506–8509.
26. Davidson,B. *et al.* (2001) Ets-1 messenger RNA expression is a novel marker of poor survival in ovarian carcinoma. *Clin. Cancer Res.*, **7**, 551–557.
27. Pande,P. *et al.* (2001) Prognostic impact of Ets-1 overexpression in betel and tobacco related oral cancer. *Cancer Detect. Prev.*, **25**, 496–501.
28. Dittmer,J. (2003) The biology of the Ets1 proto-oncogene. *Mol. Cancer*, **2**, 29.
29. Verschoor,M.L. *et al.* (2010) Ets-1 regulates energy metabolism in cancer cells. *PLoS One*, **5**, e13565.
30. Kosaka,T. *et al.* (2007) Angiotensin II type 1 receptor antagonist as an angiogenic inhibitor in prostate cancer. *Prostate*, **67**, 41–49.
31. Kosaka,T. *et al.* (2011) Phosphorylated Akt up-regulates angiotensin II type-1 receptor expression in castration resistant prostate cancer. *Prostate.*, **71**, 1510–1517.
32. Kosaka,T. *et al.* (2010) Ets-1 and hypoxia inducible factor-1alpha inhibition by angiotensin II type-1 receptor blockade in hormone-refractory prostate cancer. *Prostate*, **70**, 162–169.
33. Thalmann,G.N. *et al.* (2000) LNCaP progression model of human prostate cancer: androgen-independence and osseous metastasis. *Prostate*, **44**, 91–103. Jul 1; 44 (2).
34. Thalmann,G.N. *et al.* (1994) Androgen-independent cancer progression and bone metastasis in the LNCaP model of human prostate cancer. *Cancer Res.*, **54**, 2577–2581.
35. Wang,S. *et al.* (2003) Prostate-specific deletion of the murine Pten tumor suppressor gene leads to metastatic prostate cancer. *Cancer Cell*, **4**, 209–221.
36. Sobel,R.E. *et al.* (2005) Cell lines used in prostate cancer research: a compendium of old and new lines—part 1. *J. Urol.*, **173**, 342–359.
37. Pufall,M.A. *et al.* (2005) Variable control of Ets-1 DNA binding by multiple phosphates in an unstructured region. *Science*, **309**, 142–145.
38. Callaway,K. *et al.* (2010) Phosphorylation of the transcription factor Ets-1 by ERK2: rapid dissociation of ADP and phospho-Ets-1. *Biochemistry*, **49**, 3619–3630.
39. Tootle,T.L. *et al.* (2005) Post-translational modifications influence transcription factor activity: a view from the ETS superfamily. *Bioessays*, **27**, 285–298.
40. Foulds,C.E. *et al.* (2004) Ras/mitogen-activated protein kinase signaling activates Ets-1 and Ets-2 by CBP/p300 recruitment. *Mol. Cell Biol.*, **24**, 10954–10964.
41. Nelson,M.L. *et al.* (2010) Ras signaling requires dynamic properties of Ets1 for phosphorylation-enhanced binding to coactivator CBP. *Proc. Natl Acad. Sci. USA*, **107**, 10026–10031.
42. Shen,M.M. *et al.* (2010) Molecular genetics of prostate cancer: new prospects for old challenges. *Genes Dev.*, **24**, 1967–2000.
43. Ghosh,P.M. *et al.* (2005) Signal transduction pathways in androgen-dependent and -independent prostate cancer cell proliferation. *Endocr. Relat. Cancer*, **12**, 119–134.
44. Ghosh,P.M. *et al.* (2003) Akt in prostate cancer: possible role in androgen-independence. *Curr. Drug Metab.*, **4**, 487–496.
45. Munro,N.P. *et al.* (2010) Outcomes from Gleason 7, intermediate risk, localized prostate cancer treated with Iodine-125 monotherapy over 10 years. *Radiother. Oncol.*, **96**, 34–37.
46. Goetz,T.L. *et al.* (2000) Auto-inhibition of Ets-1 is counteracted by DNA binding cooperativity with core-binding factor alpha2. *Mol. Cell. Biol.*, **20**, 81–90.
47. Abreu-Martin,M.T. *et al.* (1999) Mitogen-activated protein kinase kinase kinase 1 activates androgen receptor-dependent transcription and apoptosis in prostate cancer. *Mol. Cell. Biol.*, **19**, 5143–5154.
48. Bakin,R.E. *et al.* (2003) Constitutive activation of the Ras/mitogen-activated protein kinase signaling pathway promotes androgen hypersensitivity in LNCaP prostate cancer cells. *Cancer Res.*, **63**, 1981–1989.
49. Franco,O.E. *et al.* (2003) Mitogen-activated protein kinase pathway is involved in androgen-independent PSA gene expression in LNCaP cells. *Prostate*, **56**, 319–325.
50. Mukherjee,R. *et al.* (2011) Upregulation of MAPK pathway is associated with survival in castrate-resistant prostate cancer. *Br. J. Cancer*, **104**, 1920–1928.
51. Gioeli,D. *et al.* (1999) Activation of mitogen-activated protein kinase associated with prostate cancer progression. *Cancer Res.*, **59**, 279–284.
52. Weinstein-Oppenheimer,C.R. *et al.* (2000) The Raf signal transduction cascade as a target for chemotherapeutic intervention in growth factor-responsive tumors. *Pharmacol. Ther.*, **88**, 229–279.
53. Kinkade,C.W. *et al.* (2008) Targeting AKT/mTOR and ERK MAPK signaling inhibits hormone-refractory prostate cancer in a preclinical mouse model. *J. Clin. Invest.*, **118**, 3051–3064.
54. Kreisberg,J.I. *et al.* (2004) Phosphorylation of Akt (Ser473) is an excellent predictor of poor clinical outcome in prostate cancer. *Cancer Res.*, **64**, 5232–5236.